State Trajectory Generation for MIMO Multirate Feedforward using Singular Value Decomposition and Time Axis Reversal

Masahiro Mae[1], Wataru Ohnishi[1] and Hiroshi Fujimoto[1]

Abstract—Multirate feedforward control provides a perfect tracking control for a desired state trajectory in ideal theoretical condition. In this study, we propose a state trajectory generation method from a desired output trajectory for a multi-input multi-output (MIMO) system using singular value decomposition and time axis reversal. This method provides perfect tracking control in MIMO systems for a desired output trajectory. We apply this method to a MIMO high-precision stage. This method improves the general applicability of multirate feedforward control for a MIMO system.

I. INTRODUCTION

Multirate feedforward control is widely used for controlling precise systems such as high-precision stages and hard disk drives [1]. Multirate feedforward control solves the problem of unstable zeros due to discretization by using zero-order hold and provides a perfect tracking control (PTC) [2]. The word "perfect tracking control" is defined as "the plant output perfectly tracks the desired trajectory with zero tracking error at every sampling point" [3].

High-precision stages are important for manufacturing semiconductors and liquid crystal panels [4]. Their demand in society is increasing annually [5]. Conventional high-precision stages have one degree of freedom (DOF) and are mechanically constrained except along the long stroke. However, demand for more precise control in recent years has spurred development of high-precision stages with six-DOFs that are lifted by air bearings [6]. These systems are controlled as a multi-input multi-output (MIMO) system. In MIMO systems, there is a coupling problem between each input and output. MIMO systems are typically controlled by a single-input single-output (SISO) controller after being decoupled with a precompensator [7]. In this method, perfect tracking control cannot be achieved because the precompensator does not consider unstable zeros due to the discretization. When a plant has unstable zeros, perfect tracking cannot be achieved by a single-rate control scheme [3]. Therefore, several studies are conducted for the approximated plant model inverse approaches in the single-rate control scheme such as nonminimum-phase zeros ignore (NPZI) method [8], zero-phase-error tracking controller (ZPETC) method [3] and zero-magnitude-error tracking controller (ZMETC) method [9]. For these reasons, a MIMO multirate feedforward controller is required for perfect tracking control in a MIMO system [10]. In multirate feedforward control for a MIMO system, the controller design is not unique because it depends

[1]The University of Tokyo, 5-1-5 Kashiwanoha, Kashiwa, Chiba, 277-8561, Japan, mmae@ieee.org, ohnishi@ieee.org, fujimoto@k.u-tokyo.ac.jp

designing a matrix B from the generalized controllability indices, and several types of controllers can be designed [11].

In multirate feedforward control, we can obtain a control input that provides perfect tracking control for a desired state trajectory [2]. Therefore, the desired state trajectory must be generated from the desired output trajectory. In conventional multirate feedforward control in the SISO system, the system is represented in a controllable canonical form and the desired state trajectory is generated by convolving the output equation using a differential relationship between the state variables [1]. In multirate forward control for a MIMO system, not all state variables can be expressed in a differential relation in some cases due to the existence of an off-diagonal term in the matrix C of the output equation. In addition, when the nominal plant has unstable zeros in continuous-time domain, the inverse system becomes unstable. Therefore, the continuous-time stable inversion [12] is studied. This method provides perfect tracking at each sampling point, but high oscillations occur in the inter-sampling behavior because this method uses the inverse of discretization zeros [13], [14]. For this reason, the independent stable inversion of unstable intrinsic and discretization zeros by a preactuation and a multirate feedforward [15] is studied. In this method, the stable inversion for the unstable intrinsic zeros is calculated using a time axis reversal and imaginary axis reversal in a continuous-time domain. Then, the stable inversion for unstable discretization zeros is calculated using a multirate feedforward. To deal with unstable intrinsic and discretization zeros separately, inter-sampling oscillations becomes smaller.

In this study, we propose a method for generating a desired state trajectory from a desired output trajectory for multirate forward control in a MIMO system using singular value decomposition. In addition, we discuss the convolution instability due to unstable zeros of the plant in continuous-time domain or several calculation errors. In these cases, we propose a calculation method that uses time axis reversal [15]. In [15], SISO systems are only considered, but in this paper, we expand a calculation method that uses time axis reversal for MIMO systems.

We focus on two-DOFs in a six-DOF high-precision stage with translation along the x axis and rotation around the y axis, which is a dual-input dual-output system with a coupling problem. We use the state trajectory generation method using singular value decomposition and time axis reversal. We also design a multirate feedforward controller for the MIMO system. We verify the effectiveness of the proposed method through simulation.

II. STATE TRAJECTORY GENERATION FOR SINGLE-INPUT SINGLE-OUTPUT SYSTEM

The conventional method for generating a desired state trajectory from a desired output trajectory in the SISO system will be described below.

The transfer function of the plant is given by

$$P(s) = \frac{B(s)}{A(s)}$$
$$= \frac{b_m s^m + b_{m-1} s^{m-1} + \cdots + b_0}{s^n + a_{n-1} s^{n-1} + \cdots + a_0}. \quad (1)$$

The state space representation of this plant in a controllable canonical form is given by

$$\frac{\mathrm{d}}{\mathrm{d}t}\begin{bmatrix} x_1(t) \\ x_2(t) \\ \vdots \\ x_n(t) \end{bmatrix} = \begin{bmatrix} 0 & 1 & \cdots & 0 \\ 0 & 0 & \cdots & 0 \\ & & \ddots & \\ -a_0 & -a_1 & \cdots & -a_{n-1} \end{bmatrix} \begin{bmatrix} x_1(t) \\ x_2(t) \\ \vdots \\ x_n(t) \end{bmatrix} + \begin{bmatrix} 0 \\ 0 \\ \vdots \\ 1 \end{bmatrix} u(t), \quad (2)$$

$$y(t) = \begin{bmatrix} b_0 & b_1 & \cdots & b_m & 0 & \cdots & 0 \end{bmatrix} \begin{bmatrix} x_1(t) \\ x_2(t) \\ \vdots \\ x_n(t) \end{bmatrix}. \quad (3)$$

Since each state variable has a differential relationship with the state equation (2), convolution of the output equation (3) in continuous-time domain gives the desired state trajectory $\boldsymbol{x}_d(t) = \begin{bmatrix} x_{1d}(t) & x_{2d}(t) & \cdots & x_{nd}(t) \end{bmatrix}^{\mathsf{T}}$ from the desired output trajectory $y_d(t)$ as

$$x_{1d}(t) = \mathcal{L}^{-1}\left[\frac{1}{b_m s^m + \cdots + b_1 s + b_0} y_d(s)\right]. \quad (4)$$

where $\mathcal{L}^{-1}$ is an inverse Laplace transform.

III. STATE TRAJECTORY GENERATION FOR MULTI-INPUT MULTI-OUTPUT SYSTEM

The proposed method of generating the state trajectory from the output trajectory in the MIMO system will be described below. In this study, the plant is assumed to be an m-input m-output nth order plant, where $m < n$ and rank($\boldsymbol{B}$) = m. This system does not have continuous-time unstable zeros.

A. Definition of multi-input multi-output system

The state equation and the output equation for an m-input m-output nth order plant are given by

$$\dot{\boldsymbol{x}}(t) = \boldsymbol{A}\boldsymbol{x}(t) + \boldsymbol{B}\boldsymbol{u}(t), \quad (5)$$
$$\boldsymbol{y}(t) = \boldsymbol{C}\boldsymbol{x}(t), \quad (6)$$

where the state variables are $\boldsymbol{x}(t) \in \mathbb{R}^{n\times1}$, each input is $\boldsymbol{u}(t) \in \mathbb{R}^{m\times1}$, each output is $\boldsymbol{y}(t) \in \mathbb{R}^{m\times1}$, and the matrices are $\boldsymbol{A} \in \mathbb{R}^{n\times n}$, $\boldsymbol{B} \in \mathbb{R}^{n\times m}$, and $\boldsymbol{C} \in \mathbb{R}^{m\times n}$.

B. Singular value decomposition for multi-input multi-output system

1) Singular value decomposition of $\boldsymbol{B}$ matrix: Singular value decomposition of the matrix $\boldsymbol{B}$ is given by

$$\boldsymbol{B} = \boldsymbol{U}\boldsymbol{\Sigma}\boldsymbol{V}^{\mathsf{H}}, \quad (7)$$

where $\boldsymbol{U} \in \mathbb{R}^{n\times n}$, $\boldsymbol{\Sigma} \in \mathbb{R}^{n\times m}$, $\boldsymbol{V} \in \mathbb{R}^{m\times m}$.

The elements of $\boldsymbol{\Sigma}$ are given by

$$\boldsymbol{\Sigma} = \begin{bmatrix} \boldsymbol{\Delta} \\ \boldsymbol{O} \end{bmatrix},$$
$$\boldsymbol{\Delta} = \mathrm{diag}(\sigma_i)\,(i = 1 \cdots m \in \mathbb{N}),$$

where $\sigma_i\,(i = 1, 2, \ldots, m \in \mathbb{N})$ are the singular values of the matrix $\boldsymbol{B}$.

Multiplying both sides of (7) by $\boldsymbol{U}^{\mathsf{H}}$ from the left yields

$$\boldsymbol{U}^{\mathsf{H}}\boldsymbol{B} = \boldsymbol{\Sigma}\boldsymbol{V}^{\mathsf{H}}$$
$$= \begin{bmatrix} \boldsymbol{\Delta}\boldsymbol{V}^{\mathsf{H}} \\ \boldsymbol{O} \end{bmatrix}. \quad (8)$$

2) Laplace transform for state equation: The Laplace transform of the state equation (5) is given by

$$s\boldsymbol{x}(s) = \boldsymbol{A}\boldsymbol{x}(s) + \boldsymbol{B}\boldsymbol{u}(s). \quad (9)$$

The state variable conversion of (9) using the transformation matrix $\boldsymbol{U}^{\mathsf{H}}$ as $\tilde{\boldsymbol{x}}(s) = \boldsymbol{U}^{\mathsf{H}}\boldsymbol{x}(s)$ is given by

$$s(\boldsymbol{U}^{\mathsf{H}}\boldsymbol{x}(s)) = (\boldsymbol{U}^{\mathsf{H}}\boldsymbol{A}\boldsymbol{U})(\boldsymbol{U}^{\mathsf{H}}\boldsymbol{x}(s)) + (\boldsymbol{U}^{\mathsf{H}}\boldsymbol{B})\boldsymbol{u}(s)$$
$$\Leftrightarrow (s\boldsymbol{I} - \boldsymbol{U}^{\mathsf{H}}\boldsymbol{A}\boldsymbol{U})\tilde{\boldsymbol{x}}(s) = (\boldsymbol{U}^{\mathsf{H}}\boldsymbol{B})\boldsymbol{u}(s)$$
$$\Leftrightarrow \boldsymbol{W}(s)\tilde{\boldsymbol{x}}(s) = \begin{bmatrix} \boldsymbol{\Delta}\boldsymbol{V}^{\mathsf{H}} \\ \boldsymbol{O} \end{bmatrix}\boldsymbol{u}(s). \quad (10)$$

$\boldsymbol{W}(s)$ of (10) is represented as

$$\boldsymbol{W}(s) = \begin{bmatrix} \boldsymbol{W}_u(s) \\ \boldsymbol{W}_l(s) \end{bmatrix}, \quad (11)$$

where $\boldsymbol{W}(s) = s\boldsymbol{I} - \boldsymbol{U}^{\mathsf{H}}\boldsymbol{A}\boldsymbol{U}$, $\boldsymbol{W}_u(s) \in \mathbb{C}^{m\times n}$, and $\boldsymbol{W}_l(s) \in \mathbb{C}^{(n-m)\times n}$.

From (10) and (11)

$$\begin{bmatrix} \boldsymbol{W}_u(s) \\ \boldsymbol{W}_l(s) \end{bmatrix}\tilde{\boldsymbol{x}}(s) = \begin{bmatrix} \boldsymbol{\Delta}\boldsymbol{V}^{\mathsf{H}} \\ \boldsymbol{O} \end{bmatrix}\boldsymbol{u}(s). \quad (12)$$

The extracted lower $(n - m)$ rows of (12) are given by

$$\boldsymbol{W}_l(s)\tilde{\boldsymbol{x}}(s) = \boldsymbol{O}. \quad (13)$$

3) Laplace transform for output equation: The Laplace transform of the output equation (6) is given by

$$\boldsymbol{y}(s) = \boldsymbol{C}\boldsymbol{x}(s). \quad (14)$$

The state variable conversion of (14) using the transformation matrix $\boldsymbol{U}^{\mathsf{H}}$ as $\tilde{\boldsymbol{x}}(s) = \boldsymbol{U}^{\mathsf{H}}\boldsymbol{x}(s)$ is given by

$$\boldsymbol{y}(s) = (\boldsymbol{C}\boldsymbol{U})(\boldsymbol{U}^{\mathsf{H}}\boldsymbol{x}(s))$$
$$\Leftrightarrow (\boldsymbol{C}\boldsymbol{U})\tilde{\boldsymbol{x}}(s) = \boldsymbol{y}(s). \quad (15)$$

4) State trajectory generation: The concatenate matrix from (13) and (15) is given by

$$\begin{bmatrix} \boldsymbol{CU} \\ \boldsymbol{W}_l(s) \end{bmatrix} \tilde{\boldsymbol{x}}(s) = \begin{bmatrix} \boldsymbol{y}(s) \\ \boldsymbol{O} \end{bmatrix}. \tag{16}$$

From (16), the state trajectory $\tilde{\boldsymbol{x}}(s)$ from the output trajectory $\boldsymbol{y}(s)$ in the MIMO system is given by

$$\tilde{\boldsymbol{x}}(s) = \begin{bmatrix} \boldsymbol{CU} \\ \boldsymbol{W}_l(s) \end{bmatrix}^{-1} \begin{bmatrix} \boldsymbol{y}(s) \\ \boldsymbol{O} \end{bmatrix}. \tag{17}$$

From the state variable conversion of (17) using the transformation matrix $\boldsymbol{U}$ as $\boldsymbol{x}(s) = \boldsymbol{U}\tilde{\boldsymbol{x}}(s)$, the state trajectory $\boldsymbol{x}(s)$ from the output trajectory $\boldsymbol{y}(s)$ in the MIMO system is given by

$$(\boldsymbol{U}\tilde{\boldsymbol{x}}(s)) = \boldsymbol{U} \begin{bmatrix} \boldsymbol{CU} \\ \boldsymbol{W}_l(s) \end{bmatrix}^{-1} \begin{bmatrix} \boldsymbol{y}(s) \\ \boldsymbol{O} \end{bmatrix}$$

$$\Leftrightarrow \boldsymbol{x}(s) = \boldsymbol{U} \begin{bmatrix} \boldsymbol{CU} \\ \boldsymbol{W}_l(s) \end{bmatrix}^{-1} \begin{bmatrix} \boldsymbol{y}(s) \\ \boldsymbol{O} \end{bmatrix}. \tag{18}$$

By inverse Laplace transform of (18), the desired state trajectory $\boldsymbol{x}_d(t)$ can be obtained from the desired output trajectory $\boldsymbol{y}_d(t)$ in the MIMO system:

$$\boldsymbol{x}_d(t) = \mathcal{L}^{-1} \left[\boldsymbol{U} \begin{bmatrix} \boldsymbol{CU} \\ \boldsymbol{W}_l(s) \end{bmatrix}^{-1} \begin{bmatrix} \boldsymbol{y}_d(s) \\ \boldsymbol{O} \end{bmatrix} \right]. \tag{19}$$

C. Time axis reversal for unstable inverse system

The desired state trajectory in (19) becomes unstable in several cases depending on whether the plant has continuous-time unstable zeros or several calculation errors. In this study, we solve this problem using the state trajectory generation method with time axis reversal [15]. We generate a stable desired state trajectory that provides perfect tracking control. In this study, it is assumed that the differential values of the desired output trajectory are given up to $n-1$ differentiations.

1) Stable-unstable decomposition: $F_{ij}(s)$ defined in (20) is decomposed into a stable part $F_{ij}^{\mathrm{st}}(s)$ and an unstable part $F_{ij}^{\mathrm{ust}}(s)$ as follows:

$$\boldsymbol{U} \begin{bmatrix} \boldsymbol{CU} \\ \boldsymbol{W}_l(s) \end{bmatrix}^{-1} = F_{ij}(s) \quad (i,j \in \{1,2,\ldots,n\}) \tag{20}$$

$$= F_{ij}^{\mathrm{st}}(s) + F_{ij}^{\mathrm{ust}}(s), \tag{21}$$

$$f_{ij}^{\mathrm{st}}(t) = \mathcal{L}^{-1} \left[F_{ij}^{\mathrm{st}}(s) \right], \tag{22}$$

$$\bar{f}_{ij}^{\mathrm{ust}}(t) = \mathcal{L}^{-1} \left[F_{ij}^{\mathrm{ust}}(-s) \right]. \tag{23}$$

Note that $F_{ij}^{\mathrm{ust}}(-s)$ is stable.

2) Stable part state trajectory generation: The desired state trajectory $\boldsymbol{x}_d^{\mathrm{st}}(t)$ for the stable part is forwardly generated as follows:

$$\boldsymbol{x}_d^{\mathrm{st}}(t) = \begin{bmatrix} x_{1d}^{\mathrm{st}}(t) & x_{2d}^{\mathrm{st}}(t) & \cdots & x_{nd}^{\mathrm{st}}(t) \end{bmatrix}^{\mathsf{T}}$$

$$= \int_{-\infty}^{t} f_{ij}^{\mathrm{st}}(t-\tau) \begin{bmatrix} \boldsymbol{y}_d(\tau) \\ \boldsymbol{O} \end{bmatrix} d\tau. \tag{24}$$

(24) can be written as

$$\boldsymbol{x}_d^{\mathrm{st}}(t) = \int_0^t f_{ij}^{\mathrm{st}}(t-\tau) \begin{bmatrix} \boldsymbol{y}_d(\tau) \\ \boldsymbol{O} \end{bmatrix} d\tau. \tag{25}$$

assuming $\boldsymbol{y}_d(t) = \boldsymbol{0}$ when $t < 0$.

3) Unstable part state trajectory generation: The desired state trajectory $\boldsymbol{x}_d^{\mathrm{ust}}$ for the unstable part is generated by

$$\boldsymbol{x}_d^{\mathrm{ust}}(t) = \begin{bmatrix} x_{1d}^{\mathrm{ust}}(t) & x_{2d}^{\mathrm{ust}}(t) & \cdots & x_{nd}^{\mathrm{ust}}(t) \end{bmatrix}^{\mathsf{T}}$$

$$= \int_{-\infty}^{\bar{t}} \bar{f}_{ij}^{\mathrm{ust}}(\bar{t} - \bar{\tau}) \begin{bmatrix} \boldsymbol{y}_d(-\bar{\tau}) \\ \boldsymbol{O} \end{bmatrix} d\bar{\tau} \Bigg|_{\bar{t}=-t}. \tag{26}$$

$\boldsymbol{x}_d^{\mathrm{ust}}$ is calculated as follows. First, a convolution between the time reversed desired output trajectory $\boldsymbol{y}_d(-\bar{t})$ and the stable signal $\bar{f}_{ij}^{\mathrm{ust}}(t)$ is calculated. Next, the time axis is reversed. A mathematical proof is provided in [16].

4) State trajectory generation from stable-unstable parts: The desired state trajectory $\boldsymbol{x}_d(t)$ is obtained by

$$\boldsymbol{x}_d(t) = \boldsymbol{x}_d^{\mathrm{st}}(t) + \boldsymbol{x}_d^{\mathrm{ust}}(t). \tag{27}$$

IV. MULTIRATE FEEDFORWARD CONTROL FOR MULTI-INPUT MULTI-OUTPUT SYSTEM

Multirate feedforward control provides PTC [2]. A digital tracking control system typically has two samplers for the reference signal $r(t)$ and the output $y(t)$, and one holder on the input $u(t)$, as shown in Fig. 1. Therefore, three time periods exist: T_r, T_y, and T_u, which represent the periods of $r(t)$, $y(t)$, and $u(t)$, respectively. A larger T_r or T_y value is defined as the frame period T_f.

A. Definition of multi-input multi-output system

In an m-input p-output nth order MIMO system, the state equation (28) and the output equation (29) describing the continuous-time plant are given by

$$\dot{\boldsymbol{x}}(t) = \boldsymbol{A}_c \boldsymbol{x}(t) + \boldsymbol{B}_c \boldsymbol{u}(t), \tag{28}$$

$$\boldsymbol{y}(t) = \boldsymbol{C}_c \boldsymbol{x}(t), \tag{29}$$

$$\boldsymbol{B}_c = \begin{bmatrix} \boldsymbol{b}_{c1} & \cdots & \boldsymbol{b}_{cm} \end{bmatrix}, \quad \boldsymbol{C}_c = \begin{bmatrix} \boldsymbol{c}_{c1} & \cdots & \boldsymbol{c}_{cp} \end{bmatrix}^{\mathsf{T}}.$$

where the plant state is $\boldsymbol{x} \in \mathbb{R}^n$, the plant input is $\boldsymbol{u} \in \mathbb{R}^m$, and the plant output is $\boldsymbol{y} \in \mathbb{R}^p$.

B. Design of $\boldsymbol{B}$ matrix from generalized controllability indices

The generalized controllability indices are defined as follows [10]:

Definition 1 (Generalized Controllability Indices): The generalized controllability indices of $(\boldsymbol{A}_c, \boldsymbol{B}_c)$ are defined below for $\boldsymbol{A}_c \in \mathbb{R}^{n \times n}$ and $\boldsymbol{B}_c = [\boldsymbol{b}_{c1}, \cdots, \boldsymbol{b}_{cm}] \in \mathbb{R}^{n \times m}$, respectively. If $(\boldsymbol{A}_c, \boldsymbol{B}_c)$ is a controllable pair, n linearly independent vectors including the linear combination can be selected from

$$\{\boldsymbol{b}_{c1}, \cdots, \boldsymbol{b}_{cm}, \boldsymbol{A}_c \boldsymbol{b}_{c1}, \cdots, \boldsymbol{A}_c \boldsymbol{b}_{cm}, \cdots, \boldsymbol{A}_c^{n-1} \boldsymbol{b}_{cm}\}.$$

Setting φ as a set of these n vectors, σ_l and N are defined by

$$\sigma_l = \mathrm{number}\{k | \boldsymbol{A}_c^{k-1} \boldsymbol{b}_{cl} \in \varphi\}, \tag{30}$$

$$\sum_{l=1}^{m} \sigma_l = n, \tag{31}$$

$$N = \max(\sigma_l). \tag{32}$$

In the MIMO system, $n (= \text{plant order})$ vectors are selected from the generalized controllability indices, and the full row rank matrix $\boldsymbol{B}$ can be designed for almost all discretized sampling periods[1]. Therefore, feedforward controllers must be designed according to their different forms.

C. Feedforward input generation from state trajectory

From (33), the control inputs $\boldsymbol{u}_{ff}[i]$ required for PTC are given by (34).

$$\boldsymbol{x}[i+1] = \boldsymbol{A}\boldsymbol{x}[i] + \boldsymbol{B}\boldsymbol{u}[i], \qquad (33)$$

$$\boldsymbol{u}_{ff}[i] = \boldsymbol{B}^{-1}(\boldsymbol{I} - z^{-1}\boldsymbol{A})\boldsymbol{x}[i+1], \qquad (34)$$

where the matrices $\boldsymbol{A}$, $\boldsymbol{x}[i]$, $\boldsymbol{u}[i]$, z and T_f are given by

$$\boldsymbol{A} = e^{\boldsymbol{A}_c T_f}, \quad \boldsymbol{x}[i] = \boldsymbol{x}(iT_f), \quad z = e^{sT_f}, \quad T_f = NT_u,$$

$$\boldsymbol{u}[i] = \begin{bmatrix} \boldsymbol{u}_1[i] & \cdots & \boldsymbol{u}_m[i] \end{bmatrix}^{\mathsf{T}}$$

$$= \begin{bmatrix} u_{11}[i] & \cdots & u_{1\sigma_1}[i] & u_{21}[i] & \cdots & u_{m\sigma_m}[i] \end{bmatrix}^{\mathsf{T}}.$$

A block diagram of the control system is shown in Fig. 1. L is a discrete-time lifting operator [17]. L^{-1} outputs the elements of the nth dimensional vector $\boldsymbol{u}_{ff}[i]$, which is input at every period T_r, in the order from 1 to n by $T_u = T_r/n$.

V. SIMULATION

A. Modeling

In the simulation, we control the fine stage of the six-DOF high-precision stage shown in Fig. 2(a). This fine stage is supported by a six-DOF air bearing gravity canceller. In this study, two-DOFs corresponding to translation x along the x axis and pitching θ_y around the y axis are controlled, as shown in Fig. 2(b).

The equations of motion for translation and pitching of the stage are given by (35) and (36) [18].

$$(M_{x1} + M_{x2})\ddot{x}_{g1} + C_{x1}\dot{x}_{g1} + K_{x1}x_{g1} + M_{x2}L_{g2}\ddot{\theta}_y = f_x \qquad (35)$$

$$(M_{x2}L_{g2}^2 + J_{\theta y})\ddot{\theta}_y + C_{\theta y}\dot{\theta}_y + K_{\theta y}\theta_y + M_{x2}L_{g2}(\ddot{x}_{g1} - g\theta_y) = \tau_y + f_x L_{fx} \qquad (36)$$

Convert x_{g1} to observable x_m by (37).

$$x_m(s) = x_{g1}(s) + L_m\theta_y(s) \qquad (37)$$

The parameters of the stage are shown in Table I.

a_{ij}, b_{ik} ($i \in \{2,4\}$, $j \in \{1,2,3,4\}$, $k \in \{1,2\}$) from the expressions (35), (36), and (37), $(\ddot{x}_m, \ddot{\theta}_y)$ explained by $(x_m, \dot{x}_m, \theta_y, \dot{\theta}_y)$ are given by (38) and (39).

$$\ddot{x}_m = a_{21}x_m + a_{22}\dot{x}_m + a_{23}\theta_y + a_{24}\dot{\theta}_y + b_{21}f_x + b_{22}\tau_y \qquad (38)$$

$$\ddot{\theta}_y = a_{41}x_m + a_{42}\dot{x}_m + a_{43}\theta_y + a_{44}\dot{\theta}_y + b_{41}f_x + b_{42}\tau_y \qquad (39)$$

The state equation (40) and the output equation (41) for the continuous-time plant are given by

$$\dot{\boldsymbol{x}}(t) = \boldsymbol{A}_c\boldsymbol{x}(t) + \boldsymbol{B}_c\boldsymbol{u}(t), \qquad (40)$$

$$\boldsymbol{y}(t) = \boldsymbol{C}_c\boldsymbol{x}(t), \qquad (41)$$

[1]This is possible because the controllability of a continuous-time system is not preserved in the discrete system only if the two poles η_i and η_j have the same real parts, and the discretizing sampling period T satisfies $\eta_i = \eta_j + j\frac{2k\pi}{T}$ ($k = \pm 1, \pm 2, \ldots$); furthermore, it is limited to only several cases.

TABLE I
MODEL PARAMETERS.

Symbol	Meaning	Value
x_m	Measured position of the fine stage	–
x_{g1}	Position of the CoG of the planar air bearing and the air gyro	–
x_{g2}	Position of the CoG of the fine stage	–
θ_y	Measured attitude angle of the fine stage	–
f_x	Input force of the fine stage in the x direction	–
τ_y	Input torque of the fine stage in the θ_y direction	–
M_{x1}	Mass of the planar air bearing and the air gyro	0.077 kg
C_{x1}	Viscosity coefficient in the x_{g1} motion	430 N/(m/s)
K_{x1}	Spring coefficient in the x_{g1} motion	11000 N/m
M_{x2}	Mass of the fine stage	5.3 kg
$J_{\theta y}$	Moment of inertia of the fine stage	0.10 kgm^2
$C_{\theta y}$	Viscosity coefficient of the fine stage in the θ_y motion	1.6 Nm/(rad/s)
$K_{\theta y}$	Spring coefficient of the fine stage in the θ_y motion	1200 Nm/rad
L_m	Distance between the measurement point of x_m and the CoR	−0.0050 m
L_{g2}	Distance between the CoR and the CoG of the fine stage	−0.051 m
L_{fx}	Distance between the CoR of the fine stage and the actuation point	−0.50 m

where the vectors $\boldsymbol{x}(t)$, $\boldsymbol{u}(t)$, and $\boldsymbol{y}(t)$, and the matrices $\boldsymbol{A}_c$, $\boldsymbol{B}_c$, and $\boldsymbol{C}_c$ are given by

$$\boldsymbol{x}(t) = \begin{bmatrix} x_m \\ \dot{x}_m \\ \theta_y \\ \dot{\theta}_y \end{bmatrix}, \quad \boldsymbol{u}(t) = \begin{bmatrix} f_x \\ \tau_y \end{bmatrix}, \quad \boldsymbol{y}(t) = \begin{bmatrix} x_m \\ \theta_y \end{bmatrix},$$

$$\boldsymbol{A}_c = \begin{bmatrix} 0 & 1 & 0 & 0 \\ a_{21} & a_{22} & a_{23} & a_{24} \\ 0 & 0 & 0 & 1 \\ a_{41} & a_{42} & a_{43} & a_{44} \end{bmatrix}, \quad \boldsymbol{C}_c = \begin{bmatrix} 1 & 0 & 0 & 0 \\ 0 & 0 & 1 & 0 \end{bmatrix},$$

$$\boldsymbol{B}_c = \begin{bmatrix} 0 & 0 \\ b_{21} & b_{22} \\ 0 & 0 \\ b_{41} & b_{42} \end{bmatrix} = \begin{bmatrix} \boldsymbol{b}_{c1} & \boldsymbol{b}_{c2} \end{bmatrix}.$$

By using the zero-order hold in the state equation (40) and the output equation (41) for the continuous-time plant with sampling period T_u, the state equation (42) and output equation (43) for the discrete-time plant are given by

$$\boldsymbol{x}[k+1] = \boldsymbol{A}_s\boldsymbol{x}[k] + \boldsymbol{B}_s\boldsymbol{u}[k], \qquad (42)$$

$$\boldsymbol{y}[k] = \boldsymbol{C}_s\boldsymbol{x}[k], \qquad (43)$$

where $\boldsymbol{x}[k]$, $\boldsymbol{u}[k]$, $\boldsymbol{y}[k]$, and $\boldsymbol{B}_s$ are given by

$$\boldsymbol{x}[k] = \begin{bmatrix} x_m[k] \\ \dot{x}_m[k] \\ \theta_y[k] \\ \dot{\theta}_y[k] \end{bmatrix}, \quad \boldsymbol{u}[k] = \begin{bmatrix} f_x[k] \\ \tau_y[k] \end{bmatrix}, \quad \boldsymbol{y}[k] = \begin{bmatrix} x_m[k] \\ \theta_y[k] \end{bmatrix},$$

$$\boldsymbol{B}_s = \begin{bmatrix} \boldsymbol{b}_{s1} & \boldsymbol{b}_{s2} \end{bmatrix}.$$

B. State trajectory generation

In this study, we use a state equation and an output equation in a balanced realization which is transformed from the state equation (42) and the output equation (43) for considering the numerical stability of the calculation in a multirate feedforward controller design. We generate a desired state trajectory from (19) using the balanced realized plant model. If the filter $F_{ij}(s)$ ($i,j \in \{1,2,\ldots,n\}$) in (20) becomes unstable, we divide it into stable and unstable parts. We generate stable desired state trajectories by adding a stable part (24) and an unstable part (26) together.
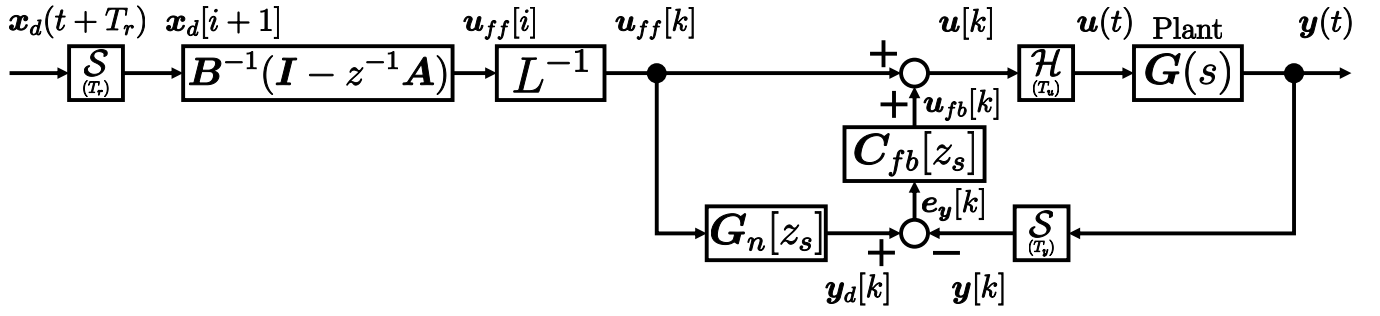
Fig. 1.   Block diagram of the controller. $\mathcal{S}$, $\mathcal{H}$, and L denote a sampler, holder, and lifting operator [17], respectively, z and z_s denote e^{sT_r} and e^{sT_u}, respectively.
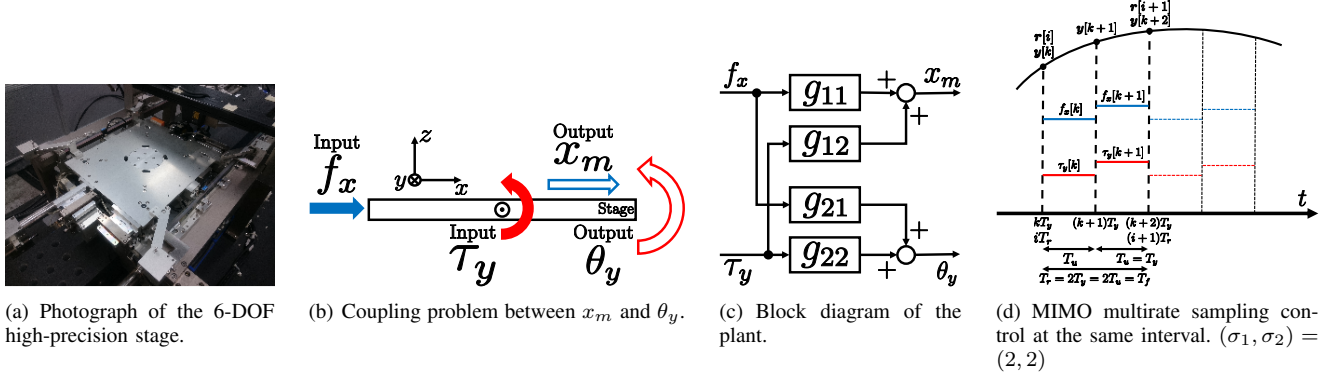

(a) Photograph of the 6-DOF high-precision stage.

(b) Coupling problem between x_m and θ_y.

(c) Block diagram of the plant.

(d) MIMO multirate sampling control at the same interval. $(\sigma_1, \sigma_2) = (2, 2)$

Fig. 2.   Simulation details.

C. Design of multirate feedforward controller for multi-input multi-output system

We design the matrix $\boldsymbol{B}$ from the generalized controllability indices:

$$\{\boldsymbol{b}_{s1}, \boldsymbol{b}_{s2}, \boldsymbol{A}_s\boldsymbol{b}_{s1}, \boldsymbol{A}_s\boldsymbol{b}_{s2}, \boldsymbol{A}_s^2\boldsymbol{b}_{s1}, \boldsymbol{A}_s^2\boldsymbol{b}_{s2}, \boldsymbol{A}_s^3\boldsymbol{b}_{s1}, \boldsymbol{A}_s^3\boldsymbol{b}_{s2}\} \quad (44)$$

In this study, we design the matrix $\boldsymbol{B}$ as follows:

$$(\sigma_1, \sigma_2) = (2, 2) : \boldsymbol{B} = \begin{bmatrix} \boldsymbol{A}_s\boldsymbol{b}_{s1} & \boldsymbol{b}_{s1} & \boldsymbol{A}_s\boldsymbol{b}_{s2} & \boldsymbol{b}_{s2} \end{bmatrix} \quad (45)$$

which is the most basic design because the number of each input is the same in the frame period T_f. These multirate inputs are shown in Fig. 2(d).

D. Condition

The trajectory x_m^{ref} is given by a seventh-order polynomial from $0\,\mu$m to $100\,\mu$m over a $0\,$ms to $20\,$ms period. The trajectory θ_y^{ref} is also given by a seventh-order polynomial from $0\,\mu$rad to $100\,\mu$rad over a $0\,$ms to $20\,$ms period. $T_u = 200\,\mu$s, $N = \max(\sigma_1, \sigma_2) = 2$ and $T_r = 2T_y = 2T_u = T_f$. The feedback controller $\boldsymbol{C}_{fb}[z_s]$ in Fig. 1 is 0 in the simulation.

E. Simulation results

The simulation results are shown in Fig. 3. Magnified views of the tracking error are shown in Fig. 4. The tracking errors become 0 at every sampling period T_f, demonstrating that perfect tracking control is achieved. Magnified views of the input in $-600\,\mu$s to $0\,\mu$s are shown in Fig. 5. Preactuation occurs at a negative time, which means that perfect tracking
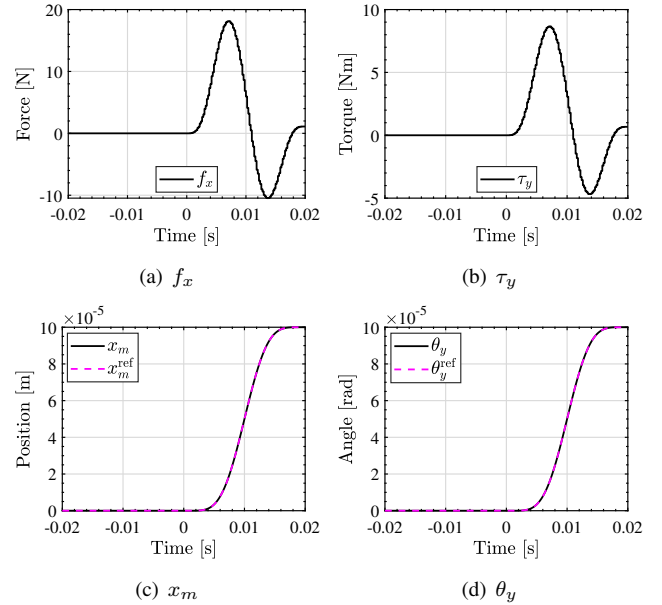

(a) f_x

(b) τ_y

(c) x_m

(d) θ_y

Fig. 3.   Simulation results of the proposed method $(\sigma_1, \sigma_2) = (2, 2)$.

control is achieved even if the inverse system is unstable. These results illustrate the effectiveness of the proposed method.

VI. CONCLUSION

In this study, we proposed a state trajectory generation method using singular value decomposition and a multirate
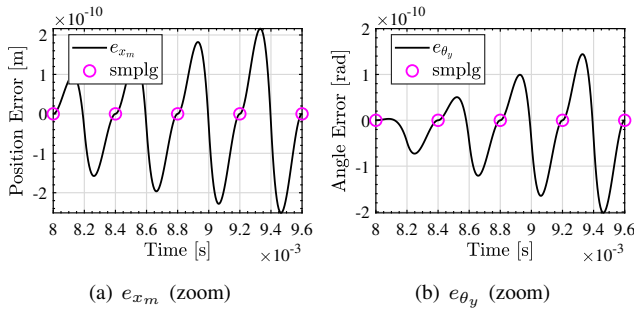
(a) e_{x_m} (zoom)

(b) e_{θ_y} (zoom)

Fig. 4. Magnified views of the tracking errors in the simulation results for the proposed method $(\sigma_1, \sigma_2) = (2, 2)$.
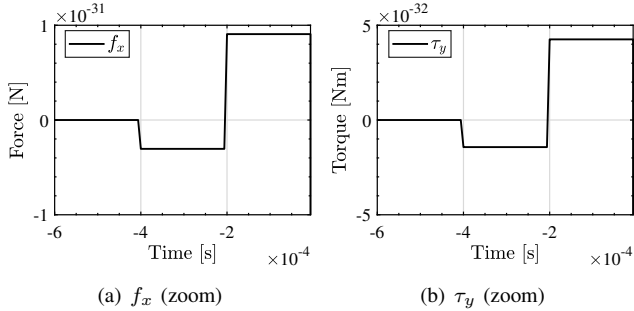

(a) f_x (zoom)

(b) τ_y (zoom)

Fig. 5. Magnified views of the inputs in the simulation results for the proposed method $(\sigma_1, \sigma_2) = (2, 2)$.

feedforward controller designed for a MIMO system. We can use a multirate feedforward controller more generally in MIMO systems using this method. We also discussed the calculation method using time axis reversal when the generated state trajectory is unstable due to unstable zeros in continuous-time domain or several calculation errors. The effectiveness of the proposed method was verified from a simulation of a dual-input dual-output high-precision stage. Future research will focus on comparing the effectiveness of the proposed method in various cases where the plant has unstable zeros.

REFERENCES

[1] W. Ohnishi and H. Fujimoto, "Review on multirate feedforward: model-inverse feedforward control for nonminumum phase systems," in *The 4th IEEJ international workshop on Sensing, Actuation, Motion Control, and Optimization (SAMCON2018)*, 2018.

[2] H. Fujimoto, Y. Hori, and A. Kawamura, "Perfect tracking control based on multirate feedforward control with generalized sampling periods," *IEEE Transactions on Industrial Electronics*, vol. 48, no. 3, pp. 636–644, jun 2001. [Online]. Available: http://ieeexplore.ieee.org/document/925591/

[3] M. Tomizuka, "Zero Phase Error Tracking Algorithm for Digital Control," *Journal of Dynamic Systems, Measurement, and Control*, vol. 109, no. 1, p. 65, 1987. [Online]. Available: http://dynamicsystems.asmedigitalcollection.asme.org/article.aspx?articleid=1403902

[4] T. Oomen, "Advanced Motion Control for Precision Mechatronics: Control, Identification, and Learning of Complex Systems," *IEEJ Journal of Industry Applications*, vol. 7, no. 2, pp. 127–140, 2018. [Online]. Available: https://www.jstage.jst.go.jp/article/ieejjia/7/2/7_127/_article

[5] G. E. Moore, "Cramming More Components Onto Integrated Circuits," *Electronics*, vol. 38, no. 8, 1965.

[6] W. Ohnishi, H. Fujimoto, K. Sakata, K. Suzuki, and K. Saiki, "Integrated design of mechanism and control for high-precision stages by the interaction index in the Direct Nyquist Array method," in *2015 American Control Conference (ACC)*. IEEE, jul 2015, pp. 2825–2830. [Online]. Available: http://ieeexplore.ieee.org/document/7171163/

[7] H. Butler, "Position Control in Lithographic Equipment [Applications of Control]," *IEEE Control Systems*, vol. 31, no. 5, pp. 28–47, oct 2011. [Online]. Available: https://ieeexplore.ieee.org/document/6021296/

[8] J. Butterworth, L. Pao, and D. Abramovitch, "Analysis and comparison of three discrete-time feedforward model-inverse control techniques for nonminimum-phase systems," *Mechatronics*, vol. 22, no. 5, pp. 577–587, aug 2012. [Online]. Available: http://linkinghub.elsevier.com/retrieve/pii/S0957415812000311https://linkinghub.elsevier.com/retrieve/pii/S0957415812000311

[9] J. Wen and B. Potsaid, "An experimental study of a high performance motion control system," in *Proceedings of the 2004 American Control Conference*, vol. 6. IEEE, 2004, pp. 5158–5163. [Online]. Available: https://ieeexplore.ieee.org/document/1384671/

[10] H. Fujimoto, "General Framework of Multirate Sampling Control and Applications to Motion Control Systems," *Doctoral Dissertation*, 2000.

[11] M. Mae, W. Ohnishi, H. Fujimoto, and Y. Hori, "Perfect Tracking Control Considering Generalized Controllability Indices and Application for High-Precision Stage in Translation and Pitching," *IEEJ Journal of Industry Applications*, vol. 8, no. 2, pp. 263–270, mar 2019. [Online]. Available: https://www.jstage.jst.go.jp/article/ieejjia/8/2/8_263/_article

[12] S. Devasia, Degang Chen, and B. Paden, "Nonlinear inversion-based output tracking," *IEEE Transactions on Automatic Control*, vol. 41, no. 7, pp. 930–942, jul 1996. [Online]. Available: http://ieeexplore.ieee.org/document/508898/

[13] K. L. Moore, S. Bhattacharyya, and M. Dahleh, "Capabilities and limitations of multirate control schemes," *Automatica*, vol. 29, no. 4, pp. 941–951, jul 1993. [Online]. Available: http://linkinghub.elsevier.com/retrieve/pii/000510989390098E

[14] T. Sogo and M. Joo, "Design of Compensators to Relocate Sampling Zeros of Digital Control Systems for DC Motors," *SICE Journal of Control, Measurement, and System Integration*, vol. 5, no. 5, pp. 283–289, 2012. [Online]. Available: http://japanlinkcenter.org/DN/JST.JSTAGE/jcmsi/5.283?lang=en&from=CrossRef&type=abstract

[15] W. Ohnishi, T. Beauduin, and H. Fujimoto, "Preactuated Multirate Feedforward Control for Independent Stable Inversion of Unstable Intrinsic and Discretization Zeros," *IEEE/ASME Transactions on Mechatronics*, pp. 1–1, 2019. [Online]. Available: https://ieeexplore.ieee.org/document/8629944/

[16] T. Sogo, "On the equivalence between stable inversion for nonminimum phase systems and reciprocal transfer functions defined by the two-sided Laplace transform," *Automatica*, vol. 46, no. 1, pp. 122–126, jan 2010. [Online]. Available: https://linkinghub.elsevier.com/retrieve/pii/S0005109809004695

[17] T. Chen and B. A. Francis, *Optimal Sampled-Data Control Systems*. London: Springer London, 1995. [Online]. Available: http://link.springer.com/10.1007/978-1-4471-3037-6

[18] W. Ohnishi, H. Fujimoto, K. Sakata, K. Suzuki, and K. Saiki, "Decoupling Control Method for High-Precision Stages using Multiple Actuators considering the Misalignment among the Actuation Point, Center of Gravity, and Center of Rotation," *IEEJ Journal of Industry Applications*, vol. 5, no. 2, pp. 141–147, 2016. [Online]. Available: https://www.jstage.jst.go.jp/article/ieejjia/5/2/5_141/_article